First Evaluation of PET-Based Human Biodistribution and Dosimetry of ^{18}F-FAZA, a Tracer for Imaging Tumor Hypoxia

Annarita Savi[1], Elena Incerti[1], Federico Fallanca[1], Valentino Bettinardi[1], Francesca Rossetti[2], Cristina Monterisi[3], Antonia Compierchio[1], Giampiero Negri[2], Piero Zannini[2], Luigi Gianolli[1], and Maria Picchio[1]

[1]Nuclear Medicine Department, IRCCS San Raffaele Scientific Institute, Milan, Italy; [2]Thoracic Surgery Department, IRCCS San Raffaele Scientific Institute, Milan, Italy; and [3]University of Milano–Bicocca, Milan, Italy

^{18}F-labeled fluoroazomycinarabinoside (^{18}F-FAZA) is a PET biomarker for noninvasive identification of regional tumor hypoxia. The aim of the present phase I study was to evaluate the biodistribution and dosimetry of ^{18}F-FAZA in non–small cell lung cancer patients. **Methods:** Five patients awaiting surgical resection of histologically proven or radiologically suspected non–small cell lung cancer were prospectively enrolled in the study. The patients underwent PET/CT after injection of 371 ± 32 MBq of ^{18}F-FAZA. The protocol consisted of a 10-min dynamic acquisition of the heart to calculate the activity in blood, followed by 4 whole-body PET/CT scans, from the vertex to the mid thigh, at 10, 60, 120, and 240 min after injection. Urine samples were collected after each imaging session and at 360 min after injection. Volumes of interest were drawn around visually identifiable source organs to generate time–activity curves. Residence times were determined from time–activity curves, and effective doses to individual organs and the whole body were calculated using OLINDA/EXM 1.2 for the standard male and female phantoms. **Results:** Blood clearance was characterized by a rapid distribution followed by first-order elimination. The highest uptake was in muscle and liver, with respective percentage injected activity (%IA) peaks of 42.7 ± 5.3 %IA and 5.5 ± 0.6 %IA. The total urinary excretion was 15 %IA. The critical organ, with the highest absorbed radiation doses, was the urinary bladder wall, at 0.047 ± 0.008 and 0.067 ± 0.007 mGy/MBq for the 2- and 4-h voiding intervals, respectively. The effective doses for the standard male and female phantoms were 0.013 ± 0.004 and 0.014 ± 0.004 mSv/MBq, respectively, depending on the voiding schedule. **Conclusion:** With respect to the available literature, the biodistribution of ^{18}F-FAZA in humans appeared to be slightly different from that in mice, with a low clearance in humans. Therefore, use of animal data may moderately underestimate radiation doses to organs in humans. Our dosimetry data showed that a 370-MBq injection of ^{18}F-FAZA is safe for clinical use, similar to other widely used PET ligands. In particular, the effective dose is not appreciably different from those obtained with other hypoxia tracers, such as ^{18}F-fluoromisonidazole.

Key Words: biodistribution; dosimetry; ^{18}F-FAZA PET; hypoxia; lung cancer

J Nucl Med 2017; 58:1224–1229
DOI: 10.2967/jnumed.113.122671

Received Nov. 2, 2016; revision accepted Jan. 12, 2017.
For correspondence or reprints contact: Maria Picchio, Nuclear Medicine Department, IRCCS San Raffaele Scientific Institute, Via Olgettina 60, 20132, Milan, Italy.
E-mail: picchio.maria@hsr.it
Published online Feb. 16, 2017.

Tumor hypoxia has been identified as a major independent prognostic factor influencing tumor progression, response to therapy, and overall survival in many malignancies (*1–3*). Various methods to measure tumor hypoxia have been proposed. However, none of the experimental in vivo methodologies (e.g., direct oxygen measurements) are currently used in cancer patients, mainly because they are invasive, technically demanding, and limited to accessible tumor sites (*4,5*).

Among the image-based modalities for hypoxia assessment, ^{18}F-fluoromisonidazole (^{18}F-FMISO) PET is one of the most extensively studied and is currently used in several cancer centers worldwide (*2,6,7*). ^{18}F-FMISO is, however, characterized by a relatively slow clearance from blood and nontarget tissues, thus resulting in low target-to-background contrast in PET images (*5*). Consequently, the next generation of nitroimidazole PET tracers, such as ^{18}F-labeled fluoroazomycinarabinoside (^{18}F-FAZA), ^{18}F-fluoroerythronitroimidazole (^{18}F-FETNIM), and ^{18}F-2-(2-nitro-1H-imidazol-1-yl)-*N*-(2,2,3,3,3-pentafluoropropyl)-acetamide (^{18}F-EF5), has been investigated and developed to achieve faster clearance and a better tumor-to-background ratio (*8*). In particular, ^{18}F-FAZA has been proposed, and its hypoxia-specific uptake mechanism has been demonstrated (*5*). The advantage of ^{18}F-FAZA over ^{18}F-FMISO seems related mainly to its kinetic properties (*9*), and it has been shown to be particularly promising for clinical purposes (*10–13*).

The safety and the feasibility of ^{18}F-FAZA PET imaging have already been investigated in cancer patients and found to be suitable for clinical detection of hypoxia (*3,10,12,14,15*). However, although estimation of the effective dose of a new agent should be mandatory to evaluate the risk–benefit ratio of medical radiation exposure, no data are yet available on the biodistribution and radiation safety of ^{18}F-FAZA in humans. The aim of the present phase I study was to determine these data using PET imaging of patients with non–small cell lung cancer.

MATERIALS AND METHODS

Subjects

Biodistribution data from 5 presurgical non–small cell lung cancer patients (2 men and 3 women; mean age, 72 y; range, 63–80 y) who underwent whole-body ^{18}F-FAZA PET/CT at the San Raffaele Scientific Institute between March and November 2015 were used for dosimetry analysis. In accord with the Declaration of Helsinki, all patients gave written informed consent before participating in the study, and the protocol was approved by the local Ethical Committee (EudraCT number 2011-002647-98).

Radiopharmaceutical Preparation

The nucleophilic substitution reaction of no-carrier-added ^{18}F-fluoride with 1-(2,3-di-*O*-acetyl-5-*O*-tosyl-D-arabinofuranosyl)-2-nitroimidazole

as precursor was performed (*16*). ^{18}F-fluoride was produced using a Cyclone 18/9 cyclotron (18 MeV; IBA Molecular) or an Eclipse RD cyclotron (11 MeV; Siemens) for irradiation of approximately 2 mL of enriched ^{18}O water (Cambridge Isotope Laboratories) through the $^{18}O(p,n)^{18}F$ nuclear reaction. The radiosynthesis of ^{18}F-FAZA was automatically performed with a TRACERlab FXF-N synthesis module (GE Healthcare). In the first step of the synthesis, ^{18}F-fluoride was separated from ^{18}O water using an anion exchange cartridge (preconditioned Sep-Pak Light QMA; ABX). To elute the ^{18}F-fluoride absorbed on the resin, a mixture of 0.5 mL of a solution of K_2CO_3 in water (6 mg/mL) and 1 mL of Kryptofix 222 (20 mg/mL; Merck) in CH_3CN was used. The solution in the reactor was then dried under vacuum at 60°C for 5 min and then at 120°C for another 5 min. Labeling was carried out using 5 mg of the precursor dissolved in 1 mL of anhydrous dimethyl sulfoxide under stirring at 100°C for 5 min. To remove acetyl groups, basic hydrolysis was achieved with 1 mL of 0.1N NaOH at 35°C in about 2 min. Neutralization was performed by adding 0.5 mL of 0.5N aqueous NaH_2PO_4. The reaction mixture was combined with 2 mL of high-performance liquid chromatography eluent (H_2O:EtOH 98:2 [v/v]) and then passed through an Al_2O_3 cartridge (Waters), where unreacted fluorine was adsorbed. The mixture was injected onto a semipreparative high-performance liquid chromatography column (Hypersil BDS C18; CPS Analitica) to separate the reaction product from other impurities. At a flow rate of 4 mL/min, the product had a retention time of about 34 min, detected with an ultraviolet detector in series with a Geiger–Müller radiodetector. The collected radiopharmaceutical was filtered using a 0.22-μm sterile filter (Minisart high-flow; Sartorius) and then diluted with 0.9% NaCl in order to have 12 mL. The overall radiosynthesis time was about 70 min. Quality controls were performed to determine the chemical, radiochemical, and radionuclidic purity of the final product. ^{18}F-FAZA was obtained with an overall radiochemical yield of 20%–25% (not decay-corrected), radiochemical purity of more than 99%, and specific activity of more than 37 GBq/μmol.

^{18}F-FAZA PET/CT Image Acquisition

^{18}F-FAZA was administered intravenously. The mean (±SD) administered activity to the 5 patients was 371 ± 32 MBq (range, 277–427 MBq). Imaging was performed using a whole-body PET/CT scanner (Discovery 690; GE Healthcare) with a 15.3-cm axial field of view. Before each emission imaging session, a whole-body low-dose CT scan was acquired for attenuation correction (120 kV, 50 mAs). The emission study started with a 10-min dynamic scan over the thorax region, including the heart. Four serial whole-body PET scans proceeding from vertex to mid thigh were acquired at 10, 60, 120, and 240 min after injection. The acquisition time for each scan was 3 min per bed position. The acquired data were iteratively reconstructed with corrections for attenuation, scatter, and randoms. Furthermore, time-of-flight information and the point-spread-function model were applied. The reconstruction protocol included 3-dimensional ordered-subsets expectation maximization, 3 iterations, 18 subsets, a gaussian transaxial postprocessing filter with a full width at half maximum of 4 mm, and a weighted axial filter of 1:4:1 (standard). Urine was collected at intervals of 0–60, 60–120, 120–240, and 240–300 min.

Activity Quantification and Dose Calculation

To evaluate the activity concentration in the blood (heart chamber), a region of interest (ROI) was drawn over the left ventricle—once reoriented along the short axis of the heart—and the time–activity curve was obtained from the 10-min dynamic imaging study and the 4 whole-body PET/CT studies. ROIs were drawn on the fused PET/CT images for organs that showed uptake of ^{18}F-FAZA, including brain, heart, lungs, liver, spleen, heart, muscle, and intestine. All ROIs were manually drawn on transverse slices of the first PET scan with reference to the slices of the CT scan. Then, the same ROIs were copied to the serially acquired images of each organ to form the time–activity curve. The total activity in the lung was calculated with exclusion of the tumor mass. The activity in the heart wall was obtained by subtracting the activity within the left ventricle. To determine uptake in muscle, an ROI was positioned over the upper leg muscle. The total activity for muscle was obtained by multiplying the cumulated activity per cubic centimeter by the skeletal mass (*17*). At each time point, the decayed radioactivity of each source organ was expressed as percentage injected activity (%IA) and plotted against time. Monoexponential and biexponential functions were iteratively fitted to the decay-corrected time–activity curve of each source

TABLE 1
Patient Characteristics

Characteristic	Data
Sex (*n*)	
Male	2
Female	3
Age (y)	
Mean	72
Range	63–80
Body weight (kg)	
Mean	60
Range	49–74
Injected dose (MBq)	
Mean ± SD	371 ± 32
Range	277–427
Histology (*n*)	
Adenocarcinoma	5
Other	0
Stage	
IA–IB	4
IIIA	1
Local extension (*n*)	
pT1–pT2	4
pT3	1
pN0	4
pN1	1
Mx	5
Grade (*n*)	
G2	3
G3	2

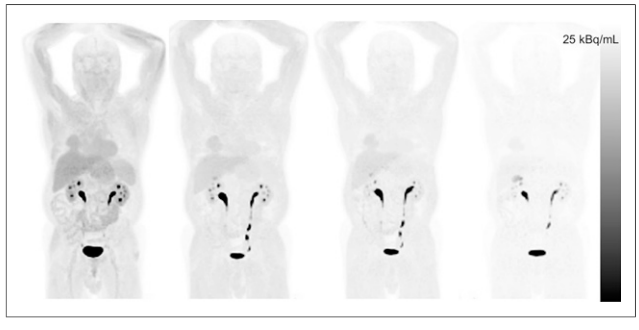

FIGURE 1. Coronal images of representative patient at 10, 60, 120, and 240 min (from left to right) after injection of ^{18}F-FAZA.

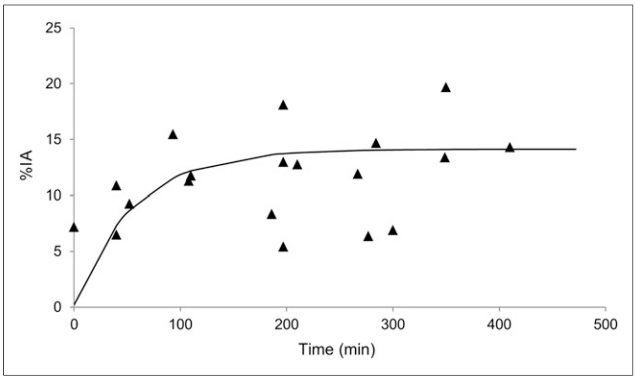

FIGURE 2. ^{18}F-FAZA urine activity expressed as %IA. Solid line represents best fit of 19 samples from 5 patients.

organ using a nonlinear least-squares regression algorithm available in MATLAB software (version 7.0; The MathWorks). For each organ, the area under each time–activity curve, from zero to infinity, was equivalent to the residence time (in hours). Because no uptake was detectable in the vertebral bodies, the cumulated activity in the red marrow was calculated by an indirect assessment of activity in the circulating blood (*18*).

Cumulative urine activity curves were generated for each patient, and the accumulated radioactivity in the urine was estimated by fitting the measured data with the empiric formula $A_u(1 - e^{-\lambda t})$, where A_u is %IA excreted in the urine and λ is the clearance rate coefficient (*19*). The residence time in the urinary bladder was determined using the dynamic bladder model in OLINDA/EXM 1.2 (Vanderbilt University, 2003) (*20*). Voiding intervals of 2 and 4 h were used to calculate different residence times and determine their effect on dose estimates to the urinary bladder wall.

Cumulated activity in the remainder of the body was calculated as follows:

$$A_{RB} = A_0 \int_0^T e^{-ln2/T_{\frac{1}{2}}t} dt + A_T \int_T^\infty e^{-ln2/T_{\frac{1}{2}}t} dt - \sum_i A_i,$$

where A_{RB} is the cumulated activity in the remainder of the body, A_0 is the injected dose, A_T is the injected dose minus the excreted activity, $T_{½}$ is the effective half-life, and A_i is the cumulated activity in the measured source organ.

The area under each time–activity curve for each organ from zero to infinity was equivalent to the residence time (in hours). The internal radiation dosimetry for each was evaluated using the MIRD schema (*21*) with OLINDA/EXM 1.2 software for the standard male and female phantoms. The effective dose and effective dose equivalent (EDE) were calculated and averaged for the 5 patients.

RESULTS

The characteristics of the patients are documented in Table 1.

Injection of ^{18}F-FAZA was well tolerated, with no pharmacologic side effects observed. Figure 1 shows a representative whole-body ^{18}F-FAZA biodistribution at various intervals after injection. At 10 min (the start time of the first whole-body acquisition), ^{18}F-FAZA uptake in this patient was seen mainly in the heart, blood, liver, spleen, urinary bladder, renal cortex, and muscle; uptake in the tumor mass of the right lung was clearly visible. Because of rapid clearance from the blood, activity was not visible in the blood or spleen on later images, whereas liver, muscle, and renal cortex were clearly visualized and contained more radioactivity than did the rest of the body.

Figure 2 shows the relative amount of ^{18}F-FAZA activity excreted in the urine. Up to 15 %IA was cleared via the urinary pathway, and this clearance was relatively rapid, with 10% of the tracer excreted 90 min after injection.

Figures 3 and 4 show the mean time–activity curves for blood, intestine, lung, brain, liver, spleen, kidneys, and muscle as derived from PET imaging of the 5 patients. Radioactivity was excreted through the kidneys, with a fast clearance and hepatic metabolism. The highest uptake was in muscle and liver, with peaks of 42.7 ± 5.3 and 5.5 ± 0.6 %IA, respectively, in the whole organ. In particular, the liver-to-muscle ratio at 10 min was approximately 2.06, whereas at 60, 120, and 240 min it was 1.47, 1.65, and 1.47, respectively.

Table 2 shows the organ residence times for ^{18}F-FAZA. The great difference in residence time between liver and muscle can be explained by the difference in mass between the two organs. For a reference human phantom of 70 kg, liver weighs only 1.9 kg whereas muscle weighs 21 or 33 kg (in the standard female and male phantoms, respectively) (*17*). Table 3 shows the radiation dose estimates. The highest absorbed radiation dose was to the urinary bladder wall, at 0.05 and 0.07 mGy/MBq for the 2- and 4-h voiding intervals, respectively. The different voiding schedules resulted in similar absorbed doses for the other organs. The effective doses were 0.013 and 0.014 mSv/MBq for the 2- and 4-h voiding intervals, respectively, resulting in respective radiation doses of 4.8 and 5.2 mSv for a 370-MBq injection of ^{18}F-FAZA.

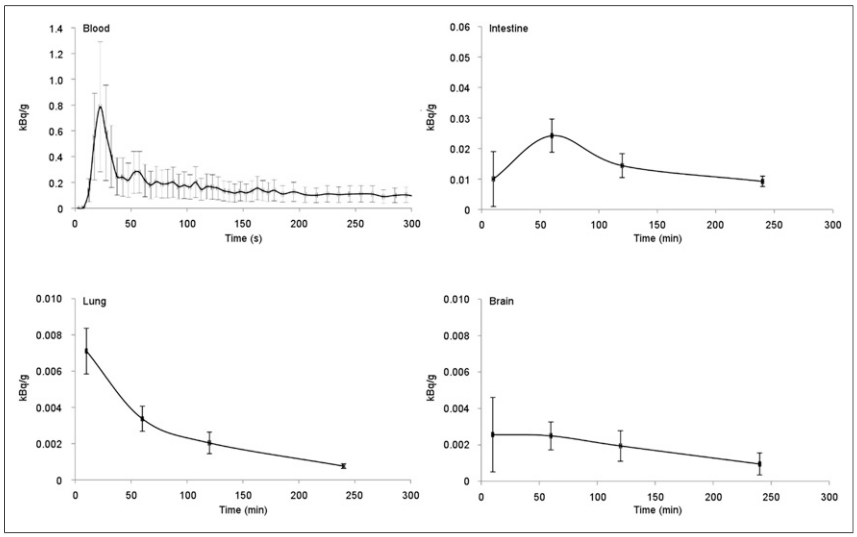

FIGURE 3. Time–activity curves for blood, intestine, lung, and brain. Activity has been normalized to 1 MBq of injected activity and standard male and female phantoms. Data represent mean ± SD of results from 5 patients.

DISCUSSION

This study was the first, to our knowledge, to determine the biodistribution and dosimetry of ^{18}F-FAZA in humans. Previously, Piert et al. (*5*) and Reischl

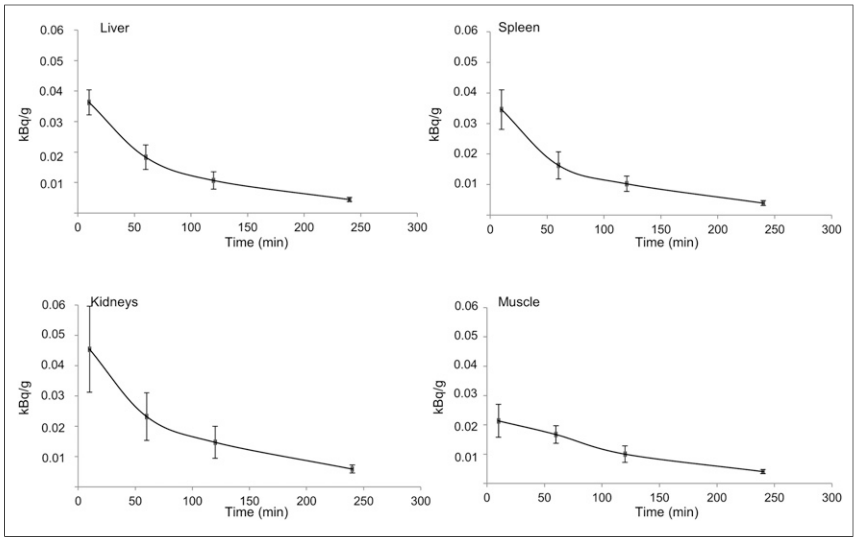

FIGURE 4. Time–activity curves in liver, spleen, kidneys, and muscle. Activity has been normalized to 1 MBq of injected activity and standard male and female phantoms. Data represent mean ± SD of results from 5 patients.

et al. (*16*) reported ^{18}F-FAZA biodistribution data for animal models, with the highest uptake being observed in liver, muscle, and kidneys and relatively lower uptake in lung, heart, muscle, and brain (*5*). These findings agree with those of the present study. However, clearance from the liver and kidney was slower in humans than in animals (half-times of 32 vs. 3 min for liver and 30 vs. 5 min for kidney), whereas clearance from muscle was comparable. The half-times in animals (nude mice) were derived from biodistribution data at 10, 60, and 180 min after administration (*5*), and the reason they were lower than in humans was probably the faster physiology of the kidneys and liver in rodents. Therefore, using data from preclinical studies may lead to an underestimation of effective dose in humans.

TABLE 2
Residence Times of ^{18}F-FAZA in Measured Source Organs

Source organ	Time
Brain	0.014 ± 0.002
Gallbladder content	0.019 ± 0.001
Intestine	0.013 ± 0.005
Heart content	0.018 ± 0.002
Kidneys	0.025 ± 0.003
Liver	0.110 ± 0.019
Lungs	0.036 ± 0.011
Muscle	1.090 ± 0.180
Red marrow	0.034 ± 0.005
Spleen	0.011 ± 0.003
Urinary bladder content at 2 h	0.055 ± 0.009
Urinary bladder content at 4 h	0.081 ± 0.008
Remainder of body at 2 h	1.130 ± 0.320
Remainder of body at 4 h	1.100 ± 0.310

Data are hours (mean ± SD; n = 5 patients).

^{18}F-FMISO, one of the first PET tracers used to image tumor oxygenation (*19*), has disadvantages such as slow accumulation, slow plasma clearance, and low tumor-to-background contrast, requiring delay of scanning (usually for more than 2 h after administration and ideally 4 h) to allow background activity to decrease (*22*). To overcome these disadvantages, other nitroimidazole PET tracers with high avidity for hypoxic tissue have been investigated and developed, including ^{18}F-FETNIM (*23*), which is more hydrophilic than ^{18}F-FMISO and washes out more rapidly from normal oxygenated tissues, theoretically allowing a higher tumor-to-background ratio (*8*). In addition, another hypoxia tracer, with a more stable but also more complex labeling chemistry, is represented by ^{18}F-EF5 (*8,24,25*). This tracer is slightly more lipophilic than the formerly described compounds and has been investigated in various tumors in animal and clinical studies (*25*). For these tracers, the optimal tumor-to-muscle cutoff is low (1.5) and the potential advantage over ^{18}F-FMISO is still negligible (*8*). When the different nitroimidazole tracers are compared, ^{18}F-FAZA, ^{18}F-EF5, and ^{18}F-FETNIM are more hydrophilic than ^{18}F-FMISO, thus diffusing into cells more quickly and being more readily available for specific reductive retention in hypoxic cells (*9,26*).

Postema et al. (*15*) provided EDE estimates for the standard male and female phantoms, as well as uptake values in various organs at 2 h after ^{18}F-FAZA administration (*5*). However, biodistribution data and doses to target organs were not reported.

In comparing our data with the available literature on ^{18}F-FMISO, ^{18}F-FETNIM, and ^{18}F-EF5 (Table 3), we found that the EDE of ^{18}F-FAZA (0.015 mSv/MBq) was slightly higher than that of ^{18}F-FMISO (0.013 mSv/MBq) (*19*). Differences in absorbed radiation dose were greatest for the urinary bladder (0.047, 0.021, 0.062, and 0.017 mGy/MBq for ^{18}F-FAZA, ^{18}F-FMISO, ^{18}F-FETNIM, and ^{18}F-EF5, respectively) because of the much higher level of urinary excretion for ^{18}F-FETNIM (60 %IA, vs. only 3, 15, and 16 %IA for ^{18}F-FMISO, ^{18}F-FAZA, and ^{18}F-EF5, respectively). We found that the EDE value for ^{18}F-FAZA (0.015 mSv/MBq) was between the values for ^{18}F-FETNIM (0.017 mSv/MBq) and ^{18}F-FMISO (0.013 mSv/MBq), whereas ^{18}F-EF5 had an EDE of 0.029 mSv/MBq. The higher doses for ^{18}F-EF5, both for urinary bladder and EDE, are probably due to the authors' assumption—in the evaluation of doses—that no activity was excreted (*25*).

^{18}F-FAZA PET/CT has also been found to be valuable as a prognostic biomarker in oncologic patients (*27*) and as a guide to tailoring treatment approaches such as hypoxia-directed intensity-modulated radiotherapy (*14,28*).

TABLE 3
Absorbed Doses of ^{18}F-FAZA to Target Organs at Various Voiding Intervals

Target organ	^{18}F-FAZA		^{18}F-FMISO at 2 h (*19*)	^{18}F-FETNIM at 2 h (*24*)	^{18}F-EF5 at 2.5 h (*26*)
	At 2 h	At 4 h			
Adrenals	0.012 ± 0.001	0.012 ± 0.001	0.017	0.012	0.014
Brain	0.004 ± 0.001	0.004 ± 0.001	0.009	0.006	0.012
Breasts	0.009 ± 0.001	0.009 ± 0.001	0.012	0.007	0.009
Gallbladder wall	0.013 ± 0.004	0.013 ± 0.004	0.015	0.014	0.055
Lower large intestine wall	0.013 ± 0.006	0.013 ± 0.006	0.014	0.012	0.017
Small intestine	0.012 ± 0.005	0.012 ± 0.005	0.013	0.012	0.015
Stomach wall	0.012 ± 0.001	0.012 ± 0.001	0.013	0.012	0.013
Upper large intestine wall	0.013 ± 0.002	0.013 ± 0.002	0.014	0.014	0.015
Heart wall	0.018 ± 0.001	0.018 ± 0.001	0.019	0.011	0.022
Kidneys	0.017 ± 0.002	0.017 ± 0.002	0.016	0.027	0.025
Liver	0.016 ± 0.003	0.016 ± 0.003	0.018	0.024	0.023
Lungs	0.011 ± 0.008	0.011 ± 0.008	0.010	0.008	0.017
Muscle	0.011 ± 0.009	0.011 ± 0.009	0.014	0.012	0.012
Ovaries	0.014 ± 0.001	0.014 ± 0.001	0.018	0.013	0.017
Pancreas	0.013 ± 0.002	0.013 ± 0.002	0.018	0.019	0.014
Red marrow	0.011 ± 0.001	0.011 ± 0.001	0.011	0.012	0.022
Bone surface	0.011 ± 0.002	0.011 ± 0.002	0.008	0.011	0.021
Skin	0.008 ± 0.001	0.008 ± 0.001	0.005	0.007	0.008
Spleen	0.017 ± 0.008	0.017 ± 0.009	0.016	0.020	0.012
Thymus	0.011 ± 0.003	0.011 ± 0.001	0.016	0.009	0.011
Thyroid	0.010 ± 0.001	0.010 ± 0.001	0.015	0.009	0.011
Urinary bladder wall	0.047 ± 0.008	0.067 ± 0.007	0.021	0.062	0.017
Uterus	0.020 ± 0.001	0.021 ± 0.001	0.018	0.015	0.023
Testes	0.004 ± 0.001	0.005 ± 0.001	0.015	0.010	0.013
Total body	0.012 ± 0.002	0.012 ± 0.002	0.013	0.011	0.014
Effective dose equivalent (mSv)	0.015 ± 0.004	0.017 ± 0.004	0.013	0.017	0.029
Effective dose (mSv)	0.013 ± 0.004	0.014 ± 0.004	—	0.015	0.023

Data are mGy/MBq (either mean or mean ± SD; $n = 5$ patients).

CONCLUSION

The biodistribution and internal dosimetry profiles for ^{18}F-FAZA in humans indicate a favorable radiation risk profile, thus making the use of whole-body ^{18}F-FAZA PET/CT feasible for evaluating clinical hypoxia and safe for consecutive studies when clinically required.

DISCLOSURE

This work was supported by the Italian Ministry of Health (Ricerca Finalizzata GR-2009-1575612). No other potential conflict of interest relevant to this article was reported.

REFERENCES

1. Cherk MH, Foo SS, Poon AM, et al. Lack of correlation of hypoxic cell fraction and angiogenesis with glucose metabolic rate in non-small cell lung cancer assessed by ^{18}F-fluoromisonidazole and ^{18}F-FDG PET. *J Nucl Med.* 2006;47:1921–1926.
2. Lewis JS, Welch MJ. PET imaging of hypoxia. *Q J Nucl Med.* 2001;45:183–188.
3. Souvatzoglou M, Grosu AL, Roper B, et al. Tumour hypoxia imaging with [^{18}F]FAZA PET in head and neck cancer patients: a pilot study. *Eur J Nucl Med Mol Imaging.* 2007;34:1566–1575.
4. Bollineni VR, Kerner GS, Pruim J, et al. PET imaging of tumor hypoxia using ^{18}F-fluoroazomycin arabinoside in stage III–IV non–small cell lung cancer patients. *J Nucl Med.* 2013;54:1175–1180.
5. Piert M, Machulla HJ, Picchio M, et al. Hypoxia-specific tumor imaging with ^{18}F-fluoroazomycin arabinoside. *J Nucl Med.* 2005;46:106–113.
6. Eschmann SM, Paulsen F, Bedeshem C, et al. Hypoxia-imaging with ^{18}F-misonidazole and PET: changes of kinetics during radiotherapy of head-and-neck cancer. *Radiother Oncol.* 2007;83:406–410.
7. Laforest R, Dehdashti F, Lewis JS, Schwarz SW. Dosimetry of $^{60/61/62/64}$Cu-ATSM: a hypoxia imaging agent for PET. *Eur J Nucl Med Mol Imaging.* 2005;32:764–770.
8. Lopci E, Grassi I, Chiti A, et al. PET radiopharmaceuticals for imaging of tumor hypoxia: a review of the evidence. *Am J Nucl Med Mol Imaging.* 2014;4:365–384.
9. Sorger D, Patt M, Kumar P, et al. [^{18}F]fluoroazomycinarabinofuranoside (^{18}FAZA) and [^{18}F]fluoromisonidazole (^{18}FMISO): a comparative study of their selective uptake in hypoxic cells and PET imaging in experimental rat tumors. *Nucl Med Biol.* 2003;30:317–326.

10. Halmos GB, Bruine de Bruin L, Langendijk JA, van der Laan BF, Pruim J, Steenbakkers RJ. Head and neck tumor hypoxia imaging by ^{18}F-fluoroazomycin-arabinoside (^{18}F-FAZA)-PET: a review. *Clin Nucl Med.* 2014;39:44–48.
11. Bollineni VR, Koole MJ, Pruim J, et al. Dynamics of tumor hypoxia assessed by ^{18}F-FAZA PET/CT in head and neck and lung cancer patients during chemoradiation: possible implications for radiotherapy treatment planning strategies. *Radiother Oncol.* 2014;113:198–203.
12. Trinkaus ME, Blum R, Rischin D, et al. Imaging of hypoxia with ^{18}F-FAZA PET in patients with locally advanced non-small cell lung cancer treated with definitive chemoradiotherapy. *J Med Imaging Radiat Oncol.* 2013;57:475–481.
13. Havelund BM, Holdgaard PC, Rafaelsen SR, et al. Tumour hypoxia imaging with ^{18}F-fluoroazomycinarabinofuranoside PET/CT in patients with locally advanced rectal cancer. *Nucl Med Commun.* 2013;34:155–161.
14. Grosu AL, Souvatzoglou M, Roper B, et al. Hypoxia imaging with FAZA-PET and theoretical considerations with regard to dose painting for individualization of radiotherapy in patients with head and neck cancer. *Int J Radiat Oncol Biol Phys.* 2007;69:541–551.
15. Postema EJ, McEwan AJ, Riauka TA, et al. Initial results of hypoxia imaging using 1-α-D-(5-deoxy-5-[^{18}F]-fluoroarabinofuranosyl)-2-nitroimidazole (^{18}F-FAZA). *Eur J Nucl Med Mol Imaging.* 2009;36:1565–1573.
16. Reischl G, Ehrlichmann W, Bieg C, et al. Preparation of the hypoxia imaging PET tracer [^{18}F]FAZA: reaction parameters and automation. *Appl Radiat Isot.* 2005;62:897–901.
17. Janssen I, Heymsfield SB, Wang ZM, Ross R. Skeletal muscle mass and distribution in 468 men and women aged 18-88 yr. *J Appl Physiol (1985).* 2000;89:81–88.
18. Sgouros G. Bone marrow dosimetry for radioimmunotherapy: theoretical considerations. *J Nucl Med.* 1993;34:689–694.
19. Graham MM, Peterson LM, Link JM, et al. Fluorine-18-fluoromisonidazole radiation dosimetry in imaging studies. *J Nucl Med.* 1997;38:1631–1636.
20. Stabin MG, Sparks RB, Crowe E. OLINDA/EXM: the second-generation personal computer software for internal dose assessment in nuclear medicine. *J Nucl Med.* 2005;46:1023–1027.
21. Stabin MG. MIRDOSE: personal computer software for internal dose assessment in nuclear medicine. *J Nucl Med.* 1996;37:538–546.
22. Yip C, Blower PJ, Goh V, Landau DB, Cook GJ. Molecular imaging of hypoxia in non-small-cell lung cancer. *Eur J Nucl Med Mol Imaging.* 2015;42:956–976.
23. Tolvanen T, Lehtio K, Kulmala J, et al. F-18-fluoroerythronitroimidazole radiation dosimetry in cancer studies. *J Nucl Med.* 2002;43:1674–1680.
24. Lin LL, Silvoniemi A, Stubbs JB, et al. Radiation dosimetry and biodistribution of the hypoxia tracer F-18-EF5 in oncologic patients. *Cancer Biother Radiopharm.* 2012;27:412–419.
25. Koch CJ, Scheuermann JS, Divgi C, et al. Biodistribution and dosimetry of F-18-EF5 in cancer patients with preliminary comparison of F-18-EF5 uptake versus EF5 binding in human glioblastoma. *Eur J Nucl Med Mol Imaging.* 2010; 37:2048–2059.
26. Kurihara H, Honda N, Kono Y, Arai Y. Radiolabelled agents for PET imaging of tumor hypoxia. *Curr Med Chem.* 2012;19:3282–3289.
27. Mortensen LS, Johansen J, Kallehauge J, et al. FAZA PET/CT hypoxia imaging in patients with squamous cell carcinoma of the head and neck treated with radiotherapy: results from the DAHANCA 24 trial. *Radiother Oncol.* 2012;105:14–20.
28. Ling CC, Humm J, Larson S, et al. Towards multidimensional radiotherapy (MD-CRT): biological imaging and biological conformality. *Int J Radiat Oncol Biol Phys.* 2000;47:551–560.